Polyhedron 229 (2023) 116193

Contents lists available at ScienceDirect

Polyhedron

journal homepage: www.elsevier.com/locate/poly

Synthesis of iridaoxaphospholane complexes

Nuria Álvarez-Pazos [a,b], Ana M. Graña [c], Jorge Bravo [a], Maria Talavera [a,*], Soledad García-Fontán [a,b,*]

[a] Departamento de Química Inorgánica, Universidade de Vigo, Campus Universitario, 36310 Vigo, Spain
[b] Metallosupramolecular Chemistry Group Galicia South Health Research Institute (IIS Galicia Sur) SERGAS-UVIGO, Galicia, Spain
[c] Departamento de Química Física, Universidade de Vigo, Campus Universitario, 36310 Vigo, Spain

ARTICLE INFO

Keywords:
Metallacycle
Oxaphosphalane
Iridium
Phosphinite ligand

ABSTRACT

An alkenylphosphinite compound has been used to synthesize the unknown iridaoxaphospholane complexes which have been characterized in solution and solid state. The reactions took place in mild conditions and the product were obtained in good yields. The synthesis of the iridaoxaphospholane complexes is based on the capability of the alkenylphosphinite compound to behave as a κ^1P or $\kappa^3(P, C, C)$ ligand when bonded to a metal complex. Theoretical calculations have been performed to explain the formation of the iridaoxaphospholane derivative due to a lower energy barrier for the nucleophilic attack at the terminal carbon of the olefin.

1. Introduction

The chemistry of metallacycles have increased enormously during the last decades due to the synergy among the organic and organometallic properties and reactivity they can display [1–5]. In this regard, iridium has emerged as one of the most promising transition metals with a wide variety of examples such as iridaaromatics [2,3,5,6], iridacyclopentadienes [7,8], iridacyclobutadienes [9] and mainly complexes bearing C—N or C—C chelating ligands [10–12], usually synthesized through C—H bond activations and presenting applications as anticancer agents, catalysts, photochemistry and in other areas [10].

Oxaphospholane compounds have risen as very important tools in enantioselective catalytic reactions due to their key role as chiral cocatalysts and the enormous demand of enantiopure products in different fields such as pharmaceutical and agrochemicals [13–16]. In this regard, different synthetic routes like dehydrohalogenation of phosphite ligands, reaction of a phosphine with a ketal or cyclocondensation reactions between phosphines and aldehydes have been developed [13,14,17,18].

Allylphosphinite ligands can coordinate with the transition metal through only the phosphorous atom κ^1P or with the additional bonding to the C═C skeleton in a $\kappa^3(P, C, C)$ coordination mode. In similar systems, this coordination mode has enabled nucleophilic addition reactions to occur involving both the C═C fragment and the metal center making possible the cyclometalation of the phosphine ligand [19–22]. In spite of the versatility of allylphosphinite ligands, they have been scarcely studied, and only have been used by García-Fontán et al. for the synthesis of rhenium carbonyl complexes $[ReX(CO)_3(P\text{-}Ph_2OCH_2CH{=}CH_2)_2]$ (X = Cl, Br) [23]. However, in that study, the allylphosphinite only acted as a κ^1P ligand and reactivity studies were not performed.

Herein, it is presented the synthesis of the first metallaoxaphospholane complexes based on the synthesis of the first iridium allylphosphinite complex through two coordination modes and its reactivity towards phosphines as nucleophiles.

2. Results and discussion

Treatment of the binuclear iridium complex $[Ir(\eta^5\text{-}C_5Me_5)Cl(\mu\text{-}Cl)]_2$ with two equivalents of the alkenyldiphenylphosphinite $PPh_2OCH_2CH{=}CH_2$ gave, after 3.5 h at room temperature the air-stable complex $[Ir(\eta^5\text{-}C_5Me_5)Cl_2(\kappa^1P\text{-}PPh_2OCH_2CH{=}CH_2)]$ (**1**) (Scheme 1). In the $^{31}P\{^1H\}$ NMR spectrum, complex **1** displays a unique peak as singlet at δ 73.1 ppm which is highly shifted compared to the free phosphinite ($\delta = +113$ ppm) [24], confirming its coordination to the iridium center. The ^1H NMR spectrum shows the most characteristic resonances of the complex belonging to the allyl moiety. Thus, there are two signals corresponding to the CH_2 olefinic group at δ 5.39 and 5.20 ppm as doublet of pseudo quartets due to the coupling to all the protons of the allylic moiety with values similar to the ones observed for the free ligand [24]. Similarly, the CH group appears at δ 5.90 ppm as a doublet of doublet of triplet of doublets with the extra coupling to the phosphorus atom of 0.8

* Corresponding authors.
E-mail addresses: matalaveran@uvigo.es (M. Talavera), sgarcia@uvigo.es (S. García-Fontán).

https://doi.org/10.1016/j.poly.2022.116193
Received 8 October 2022; Accepted 6 November 2022
Available online 9 November 2022

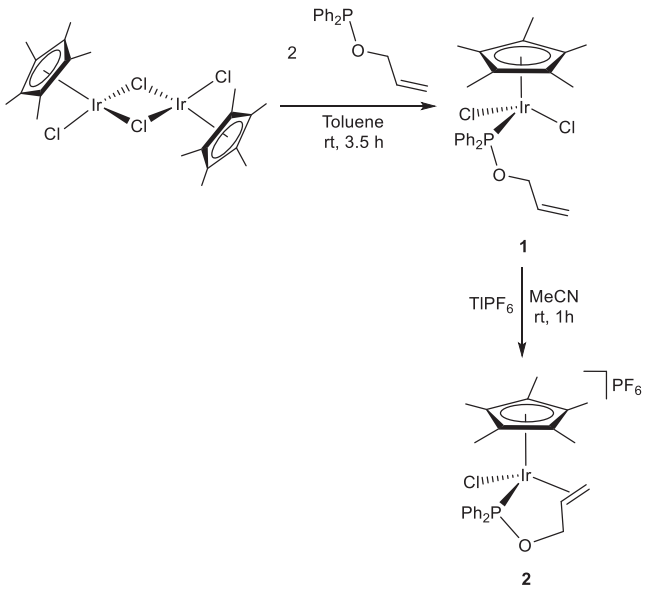

Scheme 1. Synthesis of the κ^1P and $\kappa^3(P,C,C)$ iridium complexes **1** and **2**, respectively.

Hz. Finally, the OCH_2 group appears at 4.29 ppm as a pseudo triplet of triplets with coupling to all the atoms involved. The $^{13}C\{^1H\}$ NMR spectrum displays three characteristic resonances at δ 131.2, 116.0 and 67.0 ppm for the CH, olefinic CH_2 and OCH_2 groups respectively. Note that for the two closest carbon atoms to the phosphorus atom, the signals appear as doublets due to the coupling between both nuclei. All these data are in accordance to the previously synthesized rhenium complexes bearing the allyldiphenylphosphinite ligand in κ^1P coordination mode [23].

In order to study the capability of the allyldiphenylphosphinite ligand to act as a $\kappa^3(P, C, C)$ ligand, complex **1** was treated with $TlPF_6$ in CH_3CN. Thus, the abstraction of the chlorido ligand took place, allowing the π-coordination of the allylic group to the iridium center leading to the air-stable cationic derivative $[Ir(\eta^5\text{-}C_5Me_5)Cl(\kappa^3P,C,C\text{-}PPh_2OCH_2CH{=}CH_2)][PF_6]$ (**2**) (Scheme 1). Note that the use of acetonitrile, a coordinative solvent, did not hamper the formation of **2** and no acetonitrile complex was observed as intermediate.

The change of the coordination mode is supported by the NMR spectroscopic data of complex **2**. On the one hand, the resonance of the phosphorus in the $^{31}P\{^1H\}$ NMR spectrum appears at 120 ppm, which implies a low field shift of almost 50 ppm when compared with complex **1**. On the other hand, the ^1H NMR shows five different peaks for the five protons of the allylic chain due to increase of the rigidity of the system upon coordination of the olefin to the iridium center. Therefore, the CH moiety appears as a multiplet formed by 5 doublets at δ 5.76 ppm due to the coupling to the other protons of the ligand chain and the phosphorus atom, whereas the terminal olefinic protons appear as a doublet of doublets at δ 4.71 ppm and a doublet at δ 4.14 ppm. While the former has an extra coupling to phosphorus, both resonances present couplings to the CH moiety of 8.2 and 12.6 Hz due to their *cis* and *trans* arrangement, respectively. Finally, the two OCH_2 protons appear as doublet of doublet of doublets at δ 3.76 and 4.92 ppm, where the latter shows a high increment of the proton-phosphorus coupling to 39.8 Hz, as an effect of the coordination mode change.

The presence of two diastereotopic faces would imply the formation of two diastereoisomers, however, variable temperature NMR spectroscopy studies did not show the second isomer and ruled out a possible dynamic process between them. Thus, based on the NMR data, only one of the two diastereotopic faces of the $\kappa^1P\text{-}Ph_2POCH_2CH{=}CH_2$ ligand coordinates with the metal center which implies a diastereoselective formation of complex **2**, as it has been reported for analogous compound bearing alkenylphosphane ligands [20,22,25].

The structure of compound **2** was further confirmed by X-ray diffraction studies (Fig. 1). Suitable crystals were obtained by slow diffusion of ethyl ether in a solution of compound **2** in dichloromethane. The molecule exhibits a three-legged piano-stool geometry with the iridium atom attached to the chloride ligand, the pentamethylcyclopentadienyl ring, and the alkenyldiphenylphosphinite ligand through the phosphorous and the carbon atoms of the η^2 coordinated olefin. Therefore, the bond distances between the iridium center and the olefin are 2.217(12) and 2.228(11) Å. In addition, the carbon–carbon distance of 1.4013(18) Å is larger than that found for similar complexes such as $[Ir(\eta^5\text{-}C_5Me_5)Cl(CO)(\kappa^1P\text{-}Ph_2PCH_2CH{=}CH_2)][BPh_4]$ (1.267(7) Å) [22], rhenium complexes bearing the same ligand $[ReX(CO)_3(P\text{-}Ph_2OCH_2CH{=}CH_2)_2]$ (X = Cl, Br) (around 1.32 Å) [23] or the DFT optimized structure of complex **1** (1.3353 Å) (see SI) due to the lower sp^2 character of the carbon atoms upon coordination to the metal (see Fig. 1 for distances and angles). In addition, the solid-state structure also shows a parallel orientation of the olefin with respect to the pentamethylcyclopentadienyl ring. Notably, in solution the NMR data also supported the parallel orientation of the olefin with a relative large difference between the chemical shifts of the *geminal* protons of the olefin ($\Delta\delta$ = 0.57 ppm) and a small difference between the *cis* protons ($\Delta\delta$ = 1.05 ppm). This two facts are consistent with complexes bearing an allylphosphane ligand [21,26].

In order to synthesized metallaoxaphospholanes, the electrophilicity of the olefinic moiety at the phosphinite ligand was considered and reactivity of complex **2** towards phosphines as nucleophiles was developed. Thus, triphenylphosphine, diphenylmethylphosphine and 1,3,5-triaza-7-phosphaadamantane (PTA) were used as starting materials leading, in all cases, to the formation of the air-stable iridium (III) metallacycles $[Ir(\eta^5\text{-}C_5Me_5)Cl\{\kappa^2P,C\text{-}\ PPh_2OCH_2CHCH_2(PR_3)\}](PF_6)$ (PR_3 = PPh_3 (**3a**), PPh_2Me (**3b**), PTA (**3c**)), which can be described as 1,2-iridaoxaphospholane complexes (Scheme 2).

The obtaining of complexes **3** is supported by their NMR spectroscopic data. Thus, in the $^{31}P\{^1H\}$ NMR spectrum of each complex two doublets with coupling constants around 5–6 Hz are observed, one at around 123 ppm corresponding to the phosphinite ligand and the other at 17.3, 15.9 and −48.3 ppm for the positively charged PPh_3, PPh_2Me and PTA groups, respectively. In the ^1H NMR spectra, as happened in complex **2**, the protons in both CH_2 groups are diastereotopic. While the OCH_2 moiety is not very influenced by the change in the coordination mode, the hybridation switch from Csp^2 to Csp^3 in the CH moiety

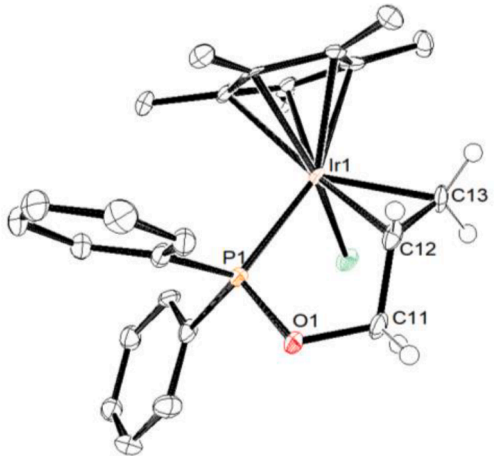

Fig. 1. ORTEP representation of complex **2** with thermal ellipsoids drawn at 50% probability level. All hydrogen atoms, except for the allylic moiety, have been omitted for clarity. Selected bond lengths (Å) and angles (°): Ir1-C12: 2.217(11); Ir1-C13: 2.228(11); Ir1-P1: 2.314(3); C12-C13: 1.415(16); C12-C11: 1.505(16); C11-O1: 1.437(12); O1-P1: 1.617(8); Ir1-P1-O1: 108.4(3); P1-O1-C11: 114.7(6); O1-C11-C12: 110.2(9); C11-C12-C13: 120.6(10).

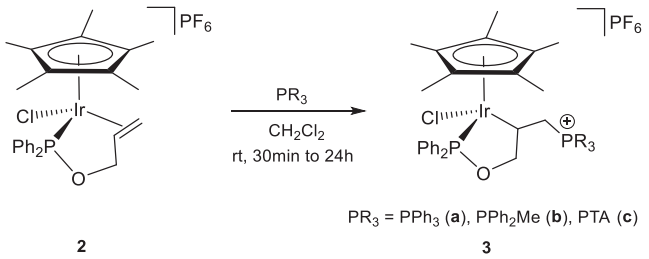

Scheme 2. Synthesis of iridaoxaphospholane complexes **3**.

produces a 2 ppm shift from 5.76 in complex **2** to around 3.45 ppm for complexes **3**. In addition, the protons of the CH_2 group bonded to the phosphane, present a doublet of doublet of doublets multiplicity in all cases with an extra coupling, compared to complex **2**, of around 15 Hz with the corresponding phosphine. Finally, the $^{13}C\{^1H\}$ NMR spectra show, not only a high field shift of the former olefinic carbons to the aliphatic region of the spectrum, but also a different multiplicity. Thus, the carbon directly bonded to the phosphine substituent appears at 25.7 ppm for **3c** as a broad signal and at 30.1 ppm for both **3a** and **3b** as doublet of doublets with couplings of around 30 Hz to the adjacent phosphorus atom and 3 Hz to the distant phosphorus nucleus. Similarly, the CH groups, now bonded to the iridium atom, show two-bond couplings of around 14 Hz for the phosphinite ligand and 5 Hz for the positively charged phosphine.

Again, the analysis in solution was further confirmed with the solid-state structure obtained by X-ray diffraction analysis of the three iridaoxaphospholanes **3** (Fig. 2 for complex **3b** and SI for the rest). The structures display a three piano legged stool geometry due to the presence of the pentamethylcyclopentadienyl and chloride ligands as well as the metallacyclic five-membered ring. Thus, the Ir—P and Ir—C distances of the iridacycle (around 2.2 and 2.1 Å respectively) shorten by 0.1 Å respect to complex **2**, probably due to the formation of the cycle, and the former C═C double bond now present a distance usual of single bonds (1.537(4)). The rest of the iridaoxaphospholane moiety present similar distances and angles in comparison with other 1,2-oxaphospholane rings [16,17]. Finally, the positively charge phosphine is bonded to the iridaoxaphospholane ring through a similar P—C bond of around 1.80 Å than the P—C distances to the phosphine substituents which are in the range of 1.7 to 1.9 Å (See Fig. 2 and Table S2 for distances and angles).

Mechanistically, complexes **3** can be obtained by the nucleophilic attack of the phosphane on the terminal carbon of the olefin with the concomitant intramolecular coordination of the inner Csp^2 carbon to the metal center. This reaction leads to the formation of a five-membered ring complex instead of six-member ring, and therefore, the obtaining of the 1,2-iridaoxaphospholane derivative. Interestingly, nucleophilic addition of phosphanes to allyl or alkenylphosphane ligands at transition metals have been previously observed, however, it had always taken place at the inner carbon of the olefin [19–22].

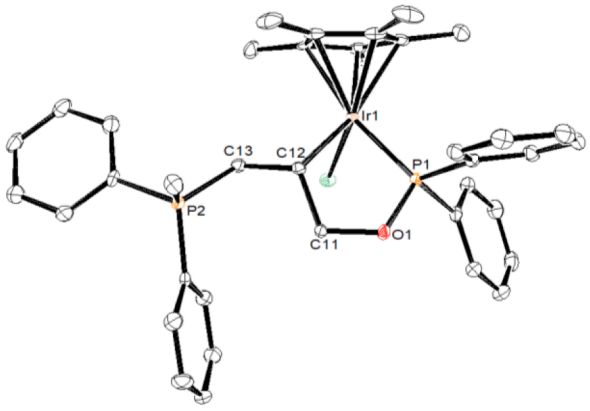

Fig. 2. ORTEP representation of cation complex **3b** with thermal ellipsoids drawn at 50% probability level. All hydrogen atoms have been omitted for clarity. Selected bond lengths (Å) and angles (°): Ir1-C12: 2.140(3); Ir1-P1: 2.2236(7); C12-C13: 1.537(4); C12-C11: 1.527(4); C11-O1: 1.455(3); O1-P1: 1.618(2); C13-P2: 1.810(3); Ir1-P1-O1: 108.87(7); P1-O1-C11: 114.42(16); O1-C11-C12: 110.8(2); C11-C12-C13: 112.0(2); C12-C13-P2: 118.77(19).

In order to shed light on the reactivity difference between the iridium (III) allylphosphine intermediate cation complex reported by Martínez de Salinas et al. $[Ir(\eta^5\text{-}C_5Me_5)Cl\{\kappa^3P,C,C\text{-}PPh_2CH_2CH{=}CH_2\}]^+$ [22] and cation complex **2**, the atomic charges of both complexes were determined by DFT calculations. Thus, the olefin of complex **2**, with a phosphinite ligand, present atomic charges of −0.07 and −0.06 au for the inner and the terminal carbon respectively, while similar values of −0.05 and −0.06 au were found for the literature described complex bearing a phosphine ligand. These results indicate that the charges have no effect in the reactivity outcome, while energy might play a role on it. Therefore, assuming a concerted mechanism for the reaction of cation complex $\mathbf{2}^+$ with PPh_2Me, the energies for the attack at both possible carbon atoms of the double bond were calculated (Fig. 3). Interestingly, the attack of the phosphine to the terminal carbon atom presents not only a lower barrier (ΔE = 8.4 kcal/mol) compared to the attack to the inner carbon atom (ΔE = 15 kcal/mol) but also, the cationic iridaoxaphospholane $\mathbf{3b}^+$ appears to be 5.2 kcal/mol more stable than the theoretical six membered ring cationic complex **3b'**.

3. Conclusions

The capability of the alkenyldiphenylphosphinite ligand to coordinate in both κ^1P and $\kappa^3(P, C, C)$ modes has allowed the synthesis of complexes $[Ir(\eta^5\text{-}C_5Me_5)Cl_2(\kappa^1P\text{-}PPh_2OCH_2CH{=}CH_2)]$ (**1**) and $[Ir(\eta^5\text{-}C_5Me_5)Cl(\kappa^3P,C,C\text{-}PPh_2OCH_2CH{=}CH_2)][PF_6]$ (**2**). Nucleophilic attack of different phosphines to the terminal carbon of the alkenyl moiety of the phosphinite ligand gave rise to a new family of metallacycles, the iridaoxaphospholane complexes $[Ir(\eta^5\text{-}C_5Me_5)Cl\{\kappa^2P,C\text{-}\ PPh_2OCH_2CH\ CH_2(PR_3)\}](PF_6)$ (PR_3 = PPh_3 (**3a**), PPh_2Me (**3b**), PTA (**3c**)). DFT calculations have determined that this reaction takes place through a lower energy barrier than a possible attack to the inner carbon as happened when using alkenylphosphane ligands.

4. Experimental section

4.1. General procedures

All synthetic procedures were performed under a dry argon atmosphere by following conventional Schlenk techniques. Solvents were purified by distillation from the appropriate drying agents and degassed before use. All reagents were obtained from commercial sources and used as received. The allyldiphenylphosphinite $PPh_2OCH_2CH{=}CH_2$ and the complex $[Ir(\eta^5\text{-}C_5Me_5)Cl(\mu\text{-}Cl)]_2$ were prepared following previously published methods [24,27]. Unless stated, NMR spectra were recorded in CD_2Cl_2 or $CDCl_3$ at room temperature on Bruker ARX–400 instrument, with resonating frequencies of 400 MHz (^1H), 161 MHz ($^{31}P\{^1H\}$), and 100 MHz ($^{13}C\{^1H\}$) using the solvent as the internal lock. ^1H and $^{13}C\{^1H\}$ signals are referred to internal TMS and those of $^{31}P\{^1H\}$ to 85 % H_3PO_4; downfield shifts (expressed in ppm) are considered positive. ^1H and $^{13}C\{^1H\}$ NMR signal assignments were confirmed by $\{^1H, ^1H\}$ COSY, $\{^1H,^{13}C\}$ HSQC and $\{^1H,^{31}P\}$ HMBC experiments. Coupling constants are given in hertz. C and H analyses were carried out with a Carlo Erba 1108 analyzer.

4.2. X-ray methodology

Crystallographic data for complexes **2, 3a**, **3b**·$2CH_2Cl_2$ and **3c** was collected on a Bruker D8 Venture Photon 100 CMOS diffractometer at 100 K using Mo-Kα radiation (λ = 0.71073 Å). The frames were

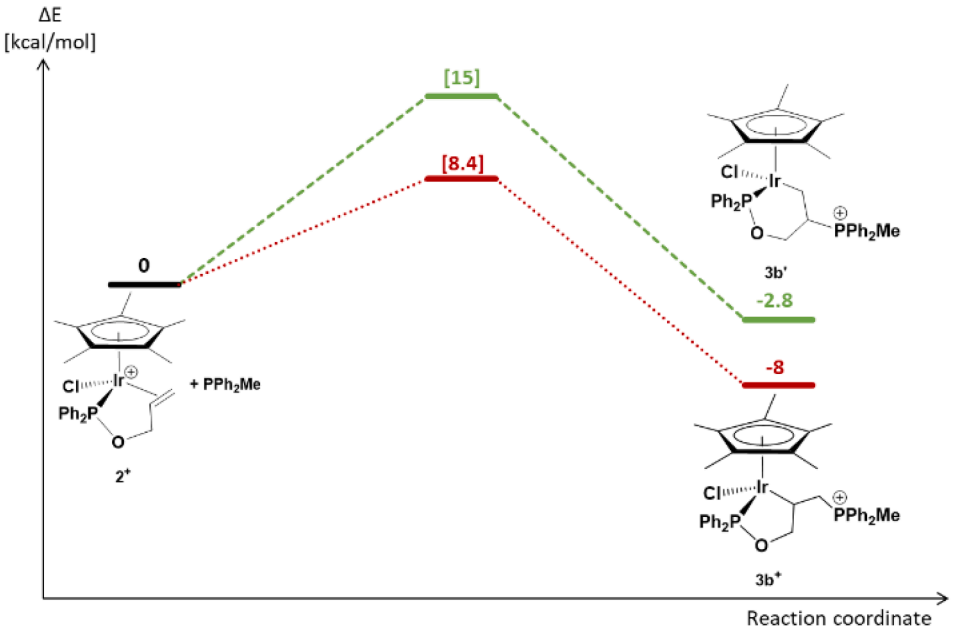

Fig. 3. Calculated energy profiles for the nucleophilic attack of PPh_2Me at the two possible positions of the coordinated olefin of $\mathbf{2}^+$. All calculated reaction and activation energies are given relative to the separate reactants $\mathbf{2}^+$ and PPh_2Me (B3LYP/Landl2DZ).

integrated with the Bruker SAINT [28] software package and the data were corrected for absorption using the program SADABS-2016/2 [29]. The structures were solved by direct methods using the program SHELXL-2019/2 [30]. All non-hydrogen atoms were refined with anisotropic thermal parameters by full-matrix least-squares calculations on F^2 using the program SHELXL-2019/2. Hydrogen atoms were inserted at calculated positions and were constrained with isotropic thermal parameters. As appear in checkcif-alerts, complexes **2** and **3c** present residual density that could not be removed but does not interfere in the structural characterization of both complexes. CCDC 2205287, 2205288, 2205289 and 2205290 contain the supplementary crystallographic data for **2**, **3a**, **3b** and **3c**, respectively. These data can be obtained free of charge from The Cambridge Crystallographic Data Centre via https://www.ccdc.cam.ac.uk/data_request/cif.

4.3. DFT calculations

All calculations were performed in the gas phase by using the B3LYP functional with the Gaussian09 package [31] and the LANL2DZ basis set. All optimized structures were characterized as critical points (minima and transition states) by using frequency calculations.

In order to obtain the values for atomic charges, a QTAIM [32] topological electron density analysis was performed on wavefunctions with the AIMAll package of programs [33].

4.4. Synthesis of compounds

4.4.1. *[Ir(η^5-C_5Me_5)Cl_2(κ^1P-$PPh_2OCH_2CH{=}CH_2$)] (**1**)*

The phosphinite $PPh_2OCH_2CH{=}CH_2$ (64 μL, 0.26 mmol) was added to a solution of $[Ir(\eta^5\text{-}C_5Me_5)Cl(\mu\text{-}Cl)]_2$ (0.10 g, 0.13 mmol) in 6 mL of toluene and stirred for 3.5 h at room temperature. Then, the mixture was concentrated under reduced pressure giving an orange oil that was treated with pentane (3 × 3 mL) and EtOH (2 × 2 mL) yielding an orange solid. Yield: 113 mg (68 %).

Elem. Anal.: Calc. for $C_{25}H_{30}Cl_2OPIr$ (640.60 g/mol): C, 46.87; H, 4.72. Exp.: C, 46.94; H, 4.81. **^{1}H NMR ($CDCl_3$)** δ: 8.16–8.02 (m, 4H, $C_{meta}H$ Ph), 7.42–7.34 (m, 6H, $C_{orto}H + C_{para}H$ Ph), 5.90 (ddtd, $^3J_{HHtrans}$ = 17.2, $^3J_{HHcis}$ = 10.4, $^3J_{HH}$ = 4.7, $^4J_{HP}$ = 0.8 Hz, 1H, $CH_2 = CH$), 5.39 (dq, $^3J_{HH}$ = 17.2, $^2J_{HH} \approx {}^4J_{HH}$ = 1.8 Hz, 1H, $=CH_2$, H_{trans}), 5.20 (dq, $^3J_{HH}$ = 10.6, $^2J_{HH} \approx {}^4J_{HH}$ = 1.7 Hz, 1H, $=CH_2$, H_{cis}), 4.29 (tt, $^3J_{HH} \approx {}^3J_{HP}$ = 4.8, $^4J_{HHcis} \approx {}^4J_{HHtrans}$ = 1.6 Hz, 2H, OCH_2), 1.44 (d, $^4J_{HP}$ = 2.5 Hz, 15H, C_5Me_5) ppm. **^{31}P {^{1}H} NMR ($CDCl_3$)** δ: 73.1 (s) ppm. **^{13}C {^{1}H} NMR (CD_2Cl_2)** δ: 136.4 (d, $^1J_{CP}$ = 60.4 Hz, C_{quat} Ph), 134.3 (d, $^4J_{CP}$ = 9.8 Hz, C_{para}H Ph), 133.1 (d, J_{CP} = 11.7 Hz, C_{orto}H Ph), 131.2 (d, $^3J_{CP}$ = 2.2 Hz, =CH), 128.0 (d, $^3J_{CP}$ = 11.1 Hz, C_{meta}H Ph), 116.0 (s, $=CH_2$), 94.6 (d, $^2J_{CP}$ = 3.0 Hz, C_5Me_5), 67.0 (d, $^2J_{CP}$ = 1.5 Hz, OCH_2), 8.3 (s, C_5Me_5) ppm.

4.4.2. *[Ir(η^5-C_5Me_5)Cl(κ^3P,C,C- $PPh_2OCH_2CH{=}CH_2$ }][PF_6] (**2**)*

A suspension of complex **1** (0.10 g, 0.15 mmol) and $TlPF_6$ (0.082 g, 0.23 mmol) in MeCN (8 mL) was stirred at room temperature for 1 h. The suspension obtained was filtered through Celite® and the filtrated was concentrated under reduced pressure giving a yellow oil that was treated with Et_2O (2 × 3 mL). The yellow solid obtained was recrystallized from a CH_2Cl_2 solution. Yield: 96 mg (85 %).

Elem. Anal.: Calc. for $C_{25}H_{30}ClF_6OP_2Ir$ (750.11 g/mol): C, 40.03; H, 4.03. Exp.: C, 40.15; H, 4.13. **^{1}H NMR (CD_2Cl_2)** δ: 7.64–7.57 (m, 2H, $C_{para}H$ Ph), 7.57–7.50 (m, 6H, C*H* Ph), 7.38–7.30 (m, 2H, C*H* Ph), 5.76 (ddddd, 1H, $^3J_{HH}$ = 12.6, $^3J_{HP}$ = 11.1, $^3J_{HH}$ = 7.9, $^4J_{HH}$ = 4.8, $^4J_{HH}$ = 2.7 Hz, =CH), 4.92 (ddd, $^3J_{HP}$ = 39.8 Hz, $^2J_{HH}$ = 10.4 Hz, $^3J_{HH}$ = 4.8 Hz, 1H, OCH_2), 4.71 (dd, $^3J_{HH}$ = 8.2 Hz, $^3J_{HP}$ = 2.5 Hz, 1H, $=CH_2$), 4.14 (d, $^3J_{HH}$ = 12.6 Hz, 1H, $=CH_2$), 3.76 (td, $^2J_{HH}$ = 10.4 Hz, $^4J_{HH}$ = 2.7 Hz, 1H, OCH_2), 1.60 (d, $^4J_{HP}$ = 2.3 Hz, 15H, C_5Me_5) ppm. **^{31}P {^{1}H} NMR (CD_2Cl_2)** δ: 120.8 (s, PO), −144.5 (sept, $^1J_{PF}$ = 710.6 Hz, PF_6) ppm. **^{13}C {^{1}H} NMR (CD_2Cl_2)** δ: 134.6 (d, $^1J_{CP}$ = 70.6 Hz, C_{quat} Ph), 133.6 (d, $^4J_{CP}$ = 2.7 Hz, C_{para}H Ph), 133.3 (d, $^4J_{CP}$ = 2.4 Hz, C_{para}H Ph), 132.9 (d, J_{CP} = 11.5 Hz, *C*H Ph), 131.8 (d, J_{CP} = 11.2 Hz, *C*H Ph), 129.6 (d, J_{CP} = 11.4 Hz, *C*H Ph), 128.9 (d, J_{CP} = 12.0 Hz, *C*H Ph), 128.4 (d, $^1J_{CP}$ = 74.1 Hz, C_{quat} Ph), 102.7 (d, $^2J_{CP}$ = 2.1 Hz, C_5Me_5), 82.8 (s br, =CH), 74.2 (s br, $=CH_2$), 71.0 (s, OCH_2), 8.8 (s, C_5Me_5) ppm.

4.4.3. *[Ir(η^5-C_5Me_5)Cl{κ^2P,C-$PPh_2OCH_2CHCH_2R$}][PF_6] (PR_3 = PPh_3 (3a), PPh_2Me (3b), PTA (**3c**))*

To a solution of the complex **2** (0.050 g, 0.06 mmol) in CH_2Cl_2 (6 mL) the corresponding phosphine was added (0.06 mmol) and the mixture stirred at room temperature for 30 min (**3a, 3b**) or 24 h (**3c**). Then, the solution was concentrated under reduced pressure giving a yellow oil that was treated with Et_2O (3 × 3 mL). The yellow solid obtained

was recrystallized from a CH_2Cl_2 solution obtaining adequate crystals for X-ray diffraction analysis. In the case of complex **3c**, the cell unit consists of two asymmetric units of the complex. Yield for **3a**: 45 mg (74 %); for **3b**: 30 mg (52 %); for **3c**: 33 mg (60 %).

Complex **3a: Elem. Anal.:** Calc. for $C_{43}H_{45}ClF_6OP_3Ir$ (1012.39 g/mol): C, 51.01; H, 4.48. Exp.: C, 51.03; H, 4.50. **^{1}H NMR (CD_2Cl_2)** δ: 7.92–7.85 (m, 3H, C$_{para}$*H* PPh$_3$), 7.79–7.72 (m, 6H, C$_{meta}$*H* PPh$_3$), 7.69–7.62 (m, 6H, C$_{orto}$*H* PPh$_3$), 7.60–7.30 (m, 8H, C*H* PPh$_2$O), 7.01–6.93 (m, 2H, C*H* PPh$_2$O), 4.39 (ddd, $^2J_{HP}$ = 15.6, $^2J_{HH}$ = 11.5, $^3J_{HH}$ = 7.0 Hz, 1H, CH$_2$P), 3.59 (ddd, $^3J_{HH}$ = 11.0, $^2J_{HH}$ = 8.9, $^3J_{HP}$ = 2.1 Hz, 1H, OCH$_2$), 3.51–3.41 (m, 1H, CH), 3.33 (ddd, $^3J_{HP}$ = 35.1, $^2J_{HH}$ = 8.9, $^3J_{HH}$ = 6.5 Hz, 1H, OCH$_2$), 3.21 (ddd, $^2J_{HP}$ = 15.2, $^2J_{HH}$ = 12.1, $^3J_{HH}$ = 2.7 Hz, 1H, CH$_2$P), 1.39 (d, $^4J_{HP}$ = 2.1 Hz, 15H, C$_5$Me$_5$) ppm; **^{31}P {^{1}H} NMR (CD_2Cl_2)** δ: 122.4 (d, $^4J_{PP}$ = 5.7 Hz, *P*Ph$_2$O), 17.3 (d, $^4J_{PP}$ = 5.5 Hz, *P*Ph$_3$), −144.5 (sept, $^1J_{PF}$ = 710.6 Hz, PF$_6$) ppm; **^{13}C {^{1}H} NMR (CD_2Cl_2)** δ: 137.3 (d, $^1J_{CP}$ = 71.7 Hz, C$_{quat}$ PPh$_2$O), 135.7 (d, $^4J_{CP}$ = 2.7 Hz, C$_{para}$H PPh$_3$), 134.1 (d, J_{CP} = 17.0 Hz, *C*H PPh$_2$O), 133.6 (d, $^2J_{CP}$ = 9.2 Hz, C$_{orto}$H PPh$_3$), 133.3 (d, J_{CP} = 12.9 Hz, *C*H PPh$_2$O), 133.1 (d, $^1J_{CP}$ = 61.6 Hz, C$_{quat}$ PPh$_2$O), 131.9 (d, $^4J_{CP}$ = 2.7 Hz, C$_{para}$H PPh$_2$O), 131.5 (d, $^4J_{CP}$ = 2.7 Hz, C$_{para}$H PPh$_2$O), 131.0 (d, $^3J_{CP}$ = 11.9 Hz, C$_{meta}$H PPh$_3$), 130.7 (d, J_{CP} = 11.0 Hz, *C*H PPh$_2$O), 128.5 (d, J_{CP} = 11.9 Hz, *C*H PPh$_2$O), 128.4 (d, J_{CP} = 11.9 Hz, *C*H PPh$_2$O), 119.2 (d, $^1J_{CP}$ = 81.8 Hz, C$_{quat}$ PPh$_3$), 94.4 (d, $^2J_{CP}$ = 3.6 Hz, *C*$_5$Me$_5$), 75.8 (dd, $^2J_{CP}$ = 3.7, $^3J_{CP}$ = 1.9 Hz, OCH$_2$), 30.1 (dd, $^1J_{CP}$ = 28.3 Hz, $^3J_{CP}$ = 3.3 Hz, CH$_2$P), 15.5 (dd, $^2J_{CP}$ = 14.5, $^2J_{CP}$ = 5.2 Hz, CH), 8.1 (s, C$_5$*Me*$_5$) ppm.

Complex **3b**: **Elem. Anal.:** Calc. for $C_{38}H_{43}ClF_6OP_3Ir$ (950.33 g/mol): C, 48.03; H, 4.56. Exp.: C, 48.23; H, 4.64. **^{1}H NMR (CD_2Cl_2)** δ: 7.86–7.75 (m, 4H, C$_{para}$*H* P*Ph*$_2$Me + C$_{para}$*H* P*Ph*$_2$O + 2C*H* P*Ph*$_2$Me), 7.75–7.63 (m, 4H, C*H* P*Ph*$_2$Me), 7.61–7.51 (m, 4H, 2C*H* PPh$_2$O + 2C*H* P*Ph*$_2$Me), 7.51–7.42 (m, 3H, 2C*H* P*Ph*$_2$O + 1C*H* P*Ph*$_2$Me), 7.42–7.36 (m, 3H, C*H* P*Ph*$_2$O), 7.11–7.01 (m, 2H, C*H* P*Ph*$_2$O), 4.13 (ddd, $^2J_{HP}$ = 15.6, $^2J_{HH}$ = 11.8, $^3J_{HH}$ = 8.1 Hz, 1H, CH$_2$P), 3.61–3.47 (m, 1H, CH), 3.35–3.26 (m, 1H, OCH$_2$), 3.24 (dm, $^3J_{HP}$ = 35.1 Hz, partially overlapped with the other OCH$_2$, 1H, OCH$_2$), 2.90 (ddd, $^2J_{HP}$ = 15.3, $^2J_{HH}$ = 11.8, $^3J_{HH}$ = 3.2 Hz, 1H, CH$_2$P), 2.54 (d, $^2J_{HP}$ = 12.7, 3H, PPh$_2$*Me*), 1.50 (d, $^4J_{HP}$ = 2.0 Hz, 15H, C$_5$Me$_5$) ppm; **^{31}P{^{1}H} NMR (CD_2Cl_2)** δ: 123.1 (d, $^4J_{PP}$ = 5.1 Hz, *P*Ph$_2$O), 15.9 (d, $^4J_{PP}$ = 4.9 Hz, *P*Ph$_2$Me), −144.3 (sept, $^1J_{PF}$ = 710.6 Hz, PF$_6$) ppm; **^{13}C {^{1}H} NMR (CD_2Cl_2)** δ: 137.4 (d, $^1J_{CP}$ = 71.7 Hz, C$_{quat}$ PPh$_2$O), 135.5 (d, $^4J_{CP}$ = 2.7 Hz, C$_{para}$H PPh$_2$Me), 135.1 (d, $^4J_{CP}$ = 2.7 Hz, C$_{para}$H PPh$_2$O), 133.31 (d, $^1J_{CP}$ = 61.6 Hz, C$_{quat}$ PPh$_2$O), 133.29 (d, J_{CP} = 11.9 Hz, *C*H PPh$_2$O), 132.3 (d, J_{CP} = 10.1 Hz, *C*H PPh$_2$Me), 131.8 (d, $^4J_{CP}$ = 2.7 Hz, C$_{para}$H PPh$_2$Me), 131.6 (d, J_{CP} = 9.2 Hz, *C*H PPh$_2$Me), 131.4 (d, $^4J_{CP}$ = 2.7 Hz, C$_{para}$H PPh$_2$O), 131.0 (d, J_{CP} = 11.9 Hz, *C*H PPh$_2$O), 130.9 (d, J_{CP} = 10.9 Hz, *C*H PPh$_2$Me), 130.8 (d, J_{CP} = 11.9 Hz, *C*H PPh$_2$Me), 128.5 (d, J_{CP} = 11.0 Hz, *C*H PPh$_2$O), 128.4 (d, J_{CP} = 11.0 Hz, *C*H PPh$_2$O), 121.9 (d, $^1J_{CP}$ = 80.0 Hz, C$_{quat}$ PPh$_2$Me), 119.8 (d, $^1J_{CP}$ = 80.9 Hz, C$_{quat}$ PPh$_2$Me), 94.4 (d, $^2J_{CP}$ = 3.7 Hz, *C*$_5$Me$_5$), 75.6 (pseudo t, $^2J_{CP}\approx{}^2J_{CP}$ = 3.5 Hz, OCH$_2$), 30.1 (dd, $^1J_{CP}$ = 30.3, $^3J_{CP}$ = 3.7 Hz, CH$_2$P), 16.0 (dd, $^2J_{CP}$ = 14.2, $^2J_{CP}$ = 5.0 Hz, CH), 8.2 (s, C$_5$*Me*$_5$), 7.4 (d, $^1J_{CP}$ = 56.1 Hz, PPh$_2$*Me*) ppm.

Complex **3c**: **Elem. Anal.:** Calc. for $C_{31}H_{42}ClF_6N_3OP_3Ir$ (907.26 g/mol): C, 41.03; H, 4.66. Exp.: C, 41.10; H, 4.71. **^{1}H NMR (CD_2Cl_2)** δ: 7.65–7.57 (m, 2H, CH_{orto} Ph$_A$), 7.54–7.47 (m, 3H, CH_{meta} + CH_{para} Ph$_A$), 7.42–7.36 (m, 3H, CH_{meta} + CH_{para} Ph$_B$), 7.13–7.06 (m, 2H, CH_{orto} Ph$_B$), 4.57–4.42 (m, 12H, CH_2 PTA), 3.68 (d pseudo t br, $^3J_{HP}$ = 32.9, $^2J_{HH}\approx{}^3J_{HH}$ = 7.0 Hz, 1H, OCH$_2$), 3.44 (ddd, $^3J_{HH}$ = 11.2, $^2J_{HH}$ = 8.2, $^3J_{HP}$ = 2.5 Hz, 1H, OCH$_2$), 3.40–3.27 (m, 1H, CH), 3.06 (ddd, $^2J_{HP}$ = 15.7, $^2J_{HH}$ = 11.2, $^3J_{HH}$ = 8.3 Hz, 1H, CH$_2$P), 2.42–2.36 (ddd, $^2J_{HP}$ = 15.5, $^2J_{HH}$ = 12.3, $^3J_{HH}$ = 3.1 Hz, 1H, CH$_2$P), 1.50 (d, $^4J_{HP}$ = 2.0 Hz, 15H, C$_5$Me$_5$) ppm; **^{31}P {^{1}H} NMR (CD_2Cl_2)** δ: 124.4 (d, $^4J_{PP}$ = 5.3 Hz, PPh$_2$O), −48.3 (d, $^4J_{PP}$ = 5.9 Hz, PTA), −144.5 (sept, $^1J_{PF}$ = 712.3 Hz, PF$_6$) ppm; **^{13}C {^{1}H} NMR (CD_2Cl_2)** δ: 133.1 (d, $^2J_{CP}$ = 12.9 Hz, C$_{orto}$H Ph$_A$), 131.8 (d, $^4J_{CP}$ = 2.2 Hz, C$_{para}$H Ph$_A$), 131.5 (d, $^4J_{CP}$ = 2.0 Hz, C$_{para}$H Ph$_B$), 131.1 (d, $^2J_{CP}$ = 11.4 Hz, C$_{orto}$H Ph$_B$), 128.5 (d, $^3J_{CP}$ = 11.2 Hz, C$_{meta}$H Ph$_A$ + Ph$_B$), 94.6 (d, $^2J_{CP}$ = 3.6 Hz, *C*$_5$Me$_5$), 76.5 (s br, OCH$_2$), 72.6 (d, $^3J_{CP}$ = 9.5 Hz, NCH$_2$N), 49.3 (d, $^1J_{CP}$ = 27.3 Hz, PCH$_2$N), 25.7 (s br, CH$_2$P), 15.3 (dd, $^2J_{CP}$ = 13.2, $^2J_{CP}$ = 4.0 Hz, CH), 8.3 (s, C$_5$*Me*$_5$) ppm. Quaternary carbon atoms of the phenyl groups could not be observed due to overlapping.

CRediT authorship contribution statement

Nuria Álvarez-Pazos: Investigation. **Ana M. Graña:** Formal analysis, Writing – review & editing. **Jorge Bravo:** Investigation, Writing – review & editing. **Maria Talavera:** Conceptualization, Writing – original draft, Writing – review & editing. **Soledad García-Fontán:** Conceptualization, Supervision, Funding acquisition, Writing – review & editing.

Declaration of Competing Interest

The authors declare that they have no known competing financial interests or personal relationships that could have appeared to influence the work reported in this paper.

Data availability

Data will be made available on request.

Acknowledgments

AMG thanks Xunta de Galicia for financial support through the project GRC2019/24. We thank the University of Vigo CACTI services for recording the NMR spectra and collecting X-ray data.

Appendix A. Supplementary data

Supplementary data to this article can be found online at https://doi.org/10.1016/j.poly.2022.116193.

References

[1] M. Albrecht, Cyclometalation using d-block transition metals: fundamental aspects and recent trends, Chem. Rev. 110 (2) (2010) 576–623.
[2] J. Chen, G. Jia, Recent development in the chemistry of transition metal-containing metallabenzenes and metallabenzynes, Coord. Chem. Rev. 257 (17) (2013) 2491–2521.
[3] B.J. Frogley, L.J. Wright, Recent advances in metallaaromatic chemistry, Chem. Eur. J. 24 (9) (2018) 2025–2038.
[4] A.P. Sadimenko, 3.19 - Five-membered rings with other elements, in: D.S. Black, J. Cossy, C.V. Stevens (Eds.), ComprehensIve Heterocyclic Chemistry IV, Elsevier, Oxford, 2022, pp. 874–1020.
[5] D. Chen, Y. Hua, H. Xia, Metallaaromatic Chemistry: History and Development, Chem. Rev. 120 (23) (2020) 12994–13086.
[6] M. Talavera, S. Bolaño, Iridaaromatics via Methoxy(alkenyl)carbeneiridium Complexes, Molecules 26 (15) (2021) 4655.
[7] R. Pereira-Cameselle, Á. Peña-Gallego, K.M. Cid-Seara, J.L. Alonso-Gómez, M. Talavera, S. Bolaño, Chemoselectivity on the synthesis of iridacycles: A theoretical and experimental study, Inorg. Chim. Acta 517 (2021), 120189.
[8] Talavera, M.; Bolaño, S.; Bravo, J.; Castro, J.; García-Fontán, S., Cyclometalated Iridium Complexes from Intramolecular C–H Activation of [IrCp*Cl{=C(OMe)CH=C(CH$_3$)R}L] (R = CH$_3$, Ph; L = PPh$_2$Me, PMe$_3$). Organometallics 2013, 32 (23), 7241-7244.
[9] G.R. Clark, G.-L. Lu, W.R. Roper, L.J. Wright, Stepwise reactions of acetylenes with iridium thiocarbonyl complexes to produce isolable iridacyclobutadienes and conversion of these to either cyclopentadienyliridium or tethered iridabenzene complexes, Organometallics 26 (9) (2007) 2167–2177.
[10] C. Michon, K. MacIntyre, Y. Corre, F. Agbossou-Niedercorn, Pentamethylcyclopentadienyl Iridium(III) metallacycles applied to homogeneous catalysis for fine chemical synthesis, ChemCatChem 8 (10) (2016) 1755–1762, and references within.
[11] C.S. Tiwari, P.M. Illam, S.N.R. Donthireddy, A. Rit, Recent advances in the syntheses and catalytic applications of homonuclear Ru-, Rh-, and Ir-complexes of CNHC^C cyclometalated ligands, Chem. Eur. J. 27 (67) (2021) 16581–16600.
[12] C. Wang, J. Xiao, Iridacycles for hydrogenation and dehydrogenation reactions, Chem. Commun. 53 (24) (2017) 3399–3411.
[13] R.A. Aitken, D.K. Sonecha, 4.16 - Five-membered rings with two nonadjacent heteroatoms with at least one phosphorus, arsenic, or antimony, in: D.S. Black, J. Cossy, C.V. Stevens (Eds.), ComprehensIve Heterocyclic Chemistry IV, Elsevier, Oxford, 2022, pp. 1061–1078.

[14] C.H. Schuster, B. Li, J.P. Morken, Modular monodentate oxaphospholane ligands: utility in highly efficient and enantioselective 1,4-diboration of 1,3-dienes, Angew. Chem. Int. Ed. 50 (34) (2011) 7906–7909.
[15] K. Huang, T.J. Emge, X. Zhang, Synthesis of a Novel P-Chiral 1,3-Oxaphospholane from Optically Pure Propylene Oxide, Heteroat. Chem 25 (2) (2014) 131–134.
[16] C.M. García, A.E. Ferao, G. Schnakenburg, R. Streubel, CPh_3 as a functional group in P-heterocyclic chemistry: elimination of $HCPh_3$ in the reaction of P-CPh3 substituted Li/Cl phosphinidenoid complexes with $Ph_2C{=}O$, Dalton Trans. 45 (6) (2016) 2378–2385.
[17] A.W. Kyri, G. Schnakenburg, R. Streubel, A novel route to C-unsubstituted 1,2-oxaphosphetane and 1,2-oxaphospholane complexes, Chem. Commun. 52 (55) (2016) 8593–8595.
[18] J.W. Heinicke, G. Thede, C. Schulzke, P.G. Jones, H. Frauendorf, PH-Functional and P-(α-hydroxy)benzyl-2-phenyl-1,3-oxaphospholanes – Synthesis, reactivity and structural aspects, Polyhedron 170 (2019) 731–741.
[19] P. Álvarez, E. Lastra, J. Gimeno, P. Braña, J.A. Sordo, J. Gomez, L.R. Falvello, M. Bassetti, Diastereoselective Synthesis of the Indenylruthenium(II) Complexes [Ru(η5-C9H7){κ3(P, C, C)-Ph2P(CH2CRCH2)}(PPh3)][PF6] (R = H, Me): Enantiofacial Coordination, Hemilabile Properties, and Diastereoselective Nucleophilic Additions to κ3(P, C, C)-Allylphosphine Ligands, Organometallics 23 (12) (2004) 2956–2966.
[20] García de la Arada, I.; Díez, J.; Gamasa, M. P.; Lastra, E., Organoruthenium complexes containing new phosphorus–carbon and phosphorus–carbon–sulfur ligands generated in the coordination sphere by nucleophilic addition reactions. Organometallics 2013, 32 (15), 4342-4352.
[21] Sánchez-Sordo, I.; Salinas, S. M. n. d.; Díez, J.; Lastra, E.; Gamasa, M. P., κ3(P,C,C)-Allylphosphane Iridium(III) and Rhodium(III) Complexes: Preparation and Reactivity toward Nucleophilic Reagents. Organometallics 2015, 34 (18), 4581-4590.
[22] S. Martínez de Salinas, I. Sánchez-Sordo, J. Díez, M. Pilar Gamasa, E. Lastra, Reactivity of κ(P)-Alkenylphosphane Rhodium(III) and Iridium(III) Complexes toward Nucleophilic Reagents, ChemistrySelect 1 (13) (2016) 4044–4051.
[23] N. Álvarez-Pazos, J. Bravo, A.M. Graña, S. García-Fontán, Rhenium(I) carbonyl complexes bearing the alkenylphosphinite ligand $Ph_2POCH_2CHCH_2$, Polyhedron 176 (2020), 114288.
[24] P.W. Clark, J.L.S. Curtis, P.E. Garrou, G.E. Hartwell, Preparation and nuclear magnetic resonance study of phosphorus compounds containing alkenyl functional groups, Can. J. Chem. 52 (9) (1974) 1714–1720.
[25] J. Díez, M.P. Gamasa, J. Gimeno, E. Lastra, A. Villar, Synthesis of New Half-Sandwich Ruthenium(II) complexes bearing alkenyl- and alkynylphosphane ligands, Eur. J. Inorg. Chem. 2006 (1) (2006) 78–87.
[26] J.W. Faller, B.V. Johnson, Organometallic conformational equilibria: XVIII. Preferred orientations and rotational barriers of π-olefins in cyclopentadienyl and indenyl complexes of iron and ruthenium, J. Organomet. Chem. 88 (1) (1975) 101–113.
[27] R.G. Ball, W.A.G. Graham, D.M. Heinekey, J.K. Hoyano, A.D. McMaster, B. M. Mattson, S.T. Michel, Synthesis and structure of dicarbonylbis(.eta.-pentamethylcyclopentadienyl)diiridium, Inorg. Chem. 29 (10) (1990) 2023–2025.
[28] Saint Data Integration software package, 6.01; Bruker Analytical X-ray Systems Inc 1997 Madison, Wisconsin, USA.
[29] Bruker AXS SADABS, Program for Empirical Absorption Correction of Area Detector Data, Madison, WI (after 2013).
[30] G. Sheldrick, Crystal structure refinement with SHELXL, Acta Crystallogr. Sect. C 71 (1) (2015) 3–8.
[31] M. J. Frisch, G. W. T., H. B. Schlegel, G. E. Scuseria, M. A. Robb, J. R. Cheeseman, G. Scalmani, V. Barone, G. A. Petersson, H. Nakatsuji, X. Li, M. Caricato, A. Marenich, J. Bloino, B. G. Janesko, R. Gomperts, B. Mennucci, H. P. Hratchian, J. V. Ortiz, A. F. Izmaylov, J. L. Sonnenberg, D. Williams-Young, F. Ding, F. Lipparini, F. Egidi, J. Goings, B. Peng, A. Petrone, T. Henderson, D. Ranasinghe, V. G. Zakrzewski, J. Gao, N. Rega, G. Zheng, W. Liang, M. Hada, M. Ehara, K. Toyota, R. Fukuda, J. Hasegawa, M. Ishida, T. Nakajima, Y. Honda, O. Kitao, H. Nakai, T. Vreven, K. Throssell, J. A. Montgomery, Jr., J. E. Peralta, F. Ogliaro, M. Bearpark, J. J. Heyd, E. Brothers, K. N. Kudin, V. N. Staroverov, T. Keith, R. Kobayashi, J. Normand, K. Raghavachari, A. Rendell, J. C. Burant, S. S. Iyengar, J. Tomasi, M. Cossi, J. M. Millam, M. Klene, C. Adamo, R. Cammi, J. W. Ochterski, R. L. Martin, K. Morokuma, O. Farkas, J. B. Foresman, and D. J. Fox *Gaussian 09*, Revision D.01; Gaussian, Inc.: Wallingford CT, 2009.
[32] R.F.W. Bader, Atoms in Molecules: A Quantum Theory, Oxford University Press, Oxford, 1990.
[33] Keith, T. A. *AIMA11*, 19.02.13; TK Gristmill Sfotw Overl Park KS: 2019.